Lasers in Manufacturing Conference 2025

Laser keyhole welding of dissimilar material combinations with complex intensity distribution

Manuel Marbach[a, 1], Jean Pierre Bergmann[b], Matthias Höbel[a]

[a]University of Applied Sciences Northwestern Switzerland FHNW, Klosterzelgstrasse 2, 5210 Windisch, Switzerland
[b]Technische Universität Ilmenau, Production Technology Group, Gustav-Kirchhoff-Platz 2, 98693 Ilmenau, Germany

Abstract

Laser keyhole welding of dissimilar materials, such as aluminum-copper (Al-Cu) and copper-steel (Cu-1.4301), is important for joining electrical components (battery to busbar). However, the joining process remains challenging due to the narrow process window and the formation of brittle intermetallic compounds (IMCs). Beam oscillation superimposed to the weld trajectory has indicated to expand the process window by modifying heat distribution and influencing IMC formation.
This study investigates the effects of spatial and temporal beam shapes created by FlexiBeam-technology. This technology utilizes a galvo scanner for non-stationary beam shaping by means of oscillation in the kilo-Hertz regime. It generates intensity distributions, such as lines, rings, rectangles, and complex patterns. Lap-joint configurations of Al-Cu and Cu-Steel1.4301 are analyzed to study weld intermixture and IMC formation. The results show that specific beam shapes improve process stability. They also reduce IMC growth, leading to better joint quality in dissimilar material welding.

Keywords: laser keyhole welding; aluminium; AW-1050A; copper; Cu-DHP; steel; 1.4301; spatial and temporal intensity shaping; velocity power control;

1. Introduction

To match the increased requirements regarding mechanical strength, weight reduction, electrical and thermal conductivity, cost and recycling, new development in material and manufacturing processes is needed. A continuous approach is being taken, to apply materials based on advantageous aspects for the product and join these dissimilar combinations. In this area, laser welding instead of mechanical fastening becomes more common, because it opens a cost-efficient path to fully automated processes to meet the named requirements.

While this application area is growing, the largest market for dissimilar laser joints is in the domain of heat exchanger manufacturing (HEM) and electric battery (EB) production (Das et al., 2018; International Energy Agency, 2023; Zwicker et al., 2020). Heat exchangers require mechanical stability over a large temperature range, while in battery production, the focus is on the reduction of the electrical contact resistance (R), whereby at the same time the mechanical integrity of the assembly must be ensured. Depending on the application, the dissimilar material combinations vary. Steel-copper is used to fix the heat exchanging elements (Cu) to the load carrying frame (stainless steel). In the production of electrical vehicles, each battery consists of a large number of battery cells. Every cell is connected to the bus bar (often an Al-Cu joint), leading to many connections for a single vehicle. Additionally, an increased research effort is invested into Steel-Aluminum connections, to reduce weight in vehicle manufacturing (Norouzian et al., 2023; Sadeghian & Iqbal, 2022).

However, dissimilar material welding is a challenge due to the variation in physical properties of the elements (Table 1). Additionally, the intermixture of the materials leads to the formation of intermetallic compounds (IMC). These IMC are brittle and have an increased hardness and increased electrical resistance (Braunovic & Alexandrov, 1994; Pfeifer et al., 2012; Ponweiser et al., 2011, 2011; Solchenbach et al., 2014; Solchenbach & Plapper, 2013). To increase the process challenges,

* Corresponding author. Tel.: +41 56 202 74 54
E-mail address: manuel.marbach@fhnw.ch

the physical properties depend on the material temperature and therefore on the local heat dissipation and thermal mass (Touloukian, 1973).

Table 1: Physical properties of materials

	Melting temperature T_{melt} [°C]	Vaporization temperature T_{vap} [°C]	Thermal conductivity κ [$W*K^{-1}*m^{-1}$]
Al (pure)	660	2520	238
AW-1050	640-655	(2520)	210
AW-5754 (AlMg3)	560-655	(2520)	140
Cu (pure)	1083	2560	397
CW024A (Cu-DHP)	1083	(2560)	305
CW008A (Cu-OF)	1083	(2560)	393
Fe (pure)	1536	2860	78
Steel 1.4301	1450	(NA)	16

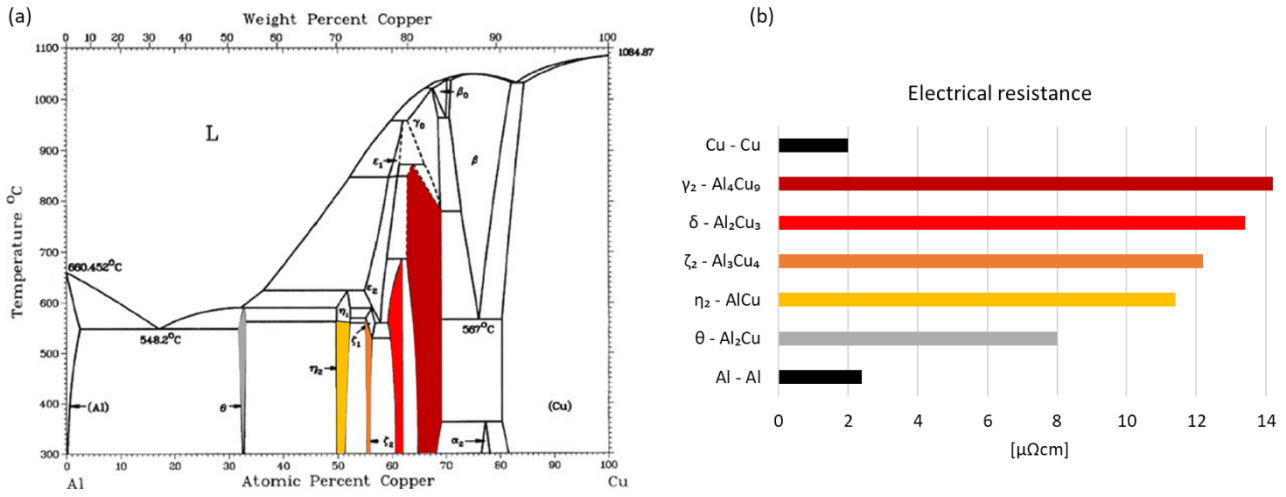

Figure 1: Intermetallic phases of Al-Cu intermixture with (a) the Al-Cu phase diagram and (b) electrical resistance (sources: Solchenbach et al., 2013 and Ponweiser et al., 2011)

To decrease the electrical resistance and maintain mechanical reliability of dissimilar joints, the IMC layer must be minimized. This is achieved by reducing the intermixture of the materials (Figure 1). The target is to remain below 33 wt% of copper in the welding zone. If this is achieved, the solidification process leads to α-aluminum and eutectic phase, which is characterized by a θ-phase with thickness <2 µm embedded in the α-aluminum. Based on the research from (Solchenbach et al., 2014), an IMC thickness <5 µm results in less than 1 µΩ electrical resistance.

When reducing the intermixture, the mechanical strength of the joint is reduced (Leitz, 2016). To ensure the joint fulfills the strength requirements of a specific application, the joining area must be increased. Such an increase is realized by beam shaping superimposed to the trajectory. Such shaping of the laser beam intensity has proven to be beneficial, and several approaches have been successfully demonstrated. A popular method is using switchable intensity distributions in fiber laser. Other methods are coherent beam combining, free form optics and fully reflective beam shaping components (Haug et al., 2019; Klocke et al., 2017; Möbus & Woizeschke, 2023; Wagner et al., 2022).

Ideally, a beam shaping system for industrial laser welding would have the capability to adapt the laser intensity distributions in a flexible manner to the application. For this purpose, more than concentric annular shapes with different distributions of energy are desirable. Beam or intensity shaping with rapid superimposed beam oscillations transverse to the trajectory can respond to that need. Using highly dynamic galvo scanners, quasi static intensity distributions can be generated. This technique can be applied to reduce pore formation and spatter during laser welding. For joining dissimilar materials, the superimposed beam oscillations can be beneficial for the reduction of intermixing material and increases the strength of the joint (Dimatteo et al., 2019; Fetzer et al., 2016; Jarwitz et al., 2018; Nahr et al., 2023; Prieto et al., 2020).

2. Experimental setup and methodology

The facility for the experiments consists of an industrial robot (ABB IRB4600-45/2.05), a processing head with integrated sensor devices and a worktop with a linear axis (Jenny Science XENAX). The robot positions the processing head over the sample. The linear axis moves the sample under the processing head with velocities up to 1500 mm/s. The energy is supplied from a single mode fiber laser (IPG YLR2000-SM) to the processing head. There, the fiber is coupled to a f70 collimator (Optoskand). The light passes the galvanometer scanner (SCANLAB excelliSCAN20) and is directed through an f250 focusing optic (Optoskand) onto the work piece.

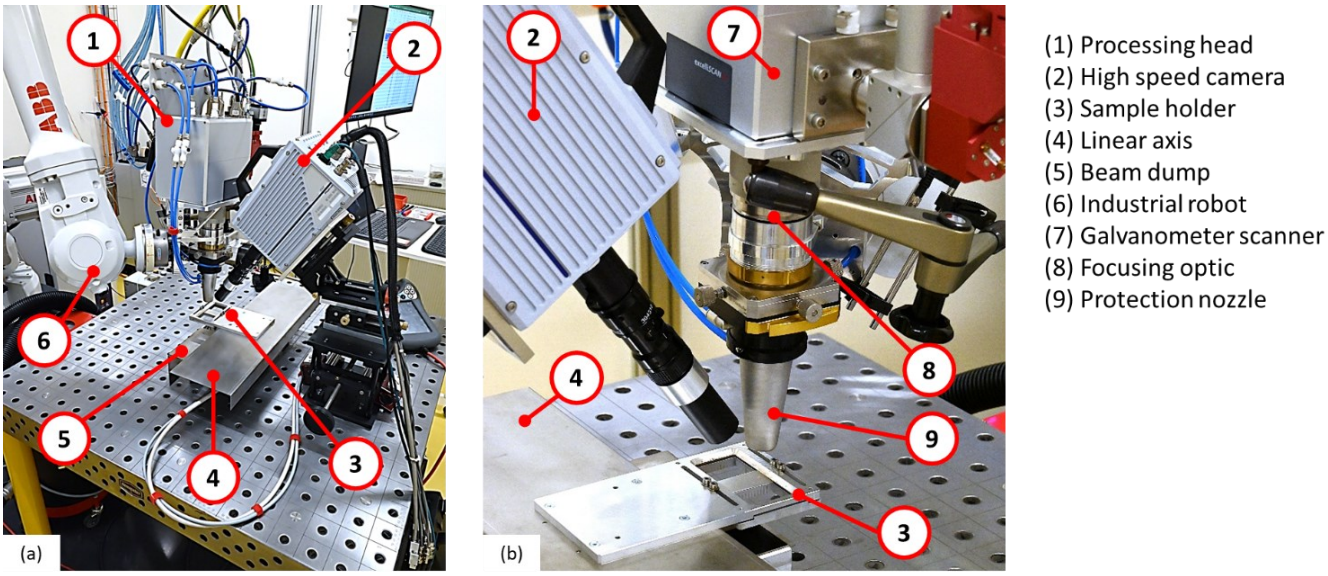

Figure 2: Setup at FHNW with (a) facility overview and (b) detail view of welding area

The optical setup results in a round laser spot of d_0=0.058 mm diameter with gaussian intensity distribution on the surface of the sample. The Rayleigh-length is z_R=2.125 mm with a beam parameter product of BPP=0.4 mm*mrad and a beam propagation ratio of M^2=1.17. The laser focus position was measured with a Cinogy beam profiler and positioned onto the surface of the samples.

The galvanometer scanner (implemented in the processing head) enables two-dimensional beam oscillation to be superimposed to the process trajectory. The system combines a 20 mm beam aperture for collimated high power laser beams. With the optical setup, the energy input into the material can be spatially and temporally modulated. By changing the amplitudes and frequencies, different oscillation figures can be created. This procedure is in detail described in an earlier contribution (Marbach et al., 2023).

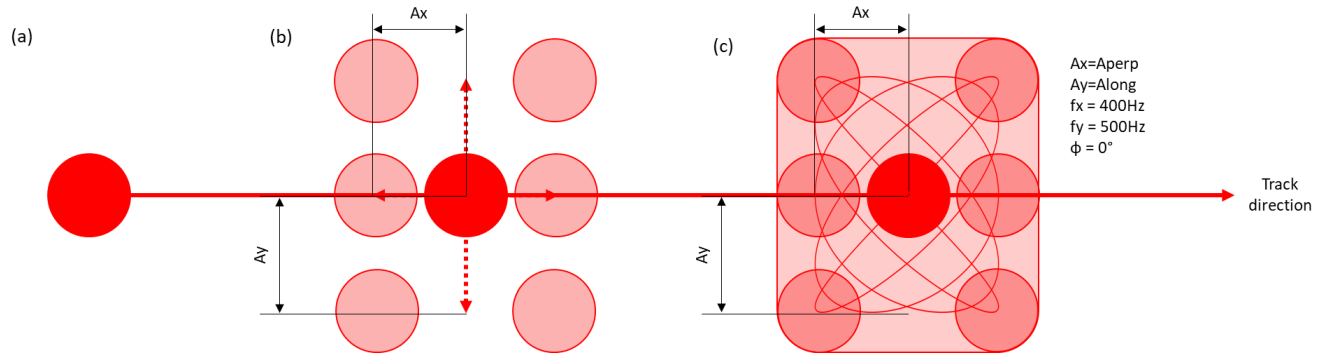

Figure 3: (a) static laser beam and trajectory; (b) visualization of amplitudes; (c) trajectory, amplitudes and frequencies combined

These dynamic beam deflections are realized as 2D harmonic oscillations. At defined frequency ratios and phase shifts, characteristic oscillation patterns are generated (so called Lissajous figures). The harmonic oscillation results in a permanent acceleration and deceleration of the laser beam during the movement along the oscillation path. When the velocity of the laser beam changes, the interaction time between the laser spot and the material changes. This has a direct effect on the process. The beam velocity is a superposition of the linear translation of the laser head and the superimposed harmonic oscillation. If the linear movement is at a velocity v_f in x-direction, the resulting velocities are shown in equation 1 and figure 4.

Equation 1: Velocity calculation for defined position

$$v_x(t) = \dot{x}(t) = v_f + 2\pi * f_{s,x} * A_{s,x} * \cos(2\pi * f_{s,x} * t * \varphi_x)$$
$$v_y(t) = \dot{y}(t) = 2\pi * f_{s,y} * A_{s,y} * \cos(2\pi * f_{s,y} * t * \varphi_y)$$

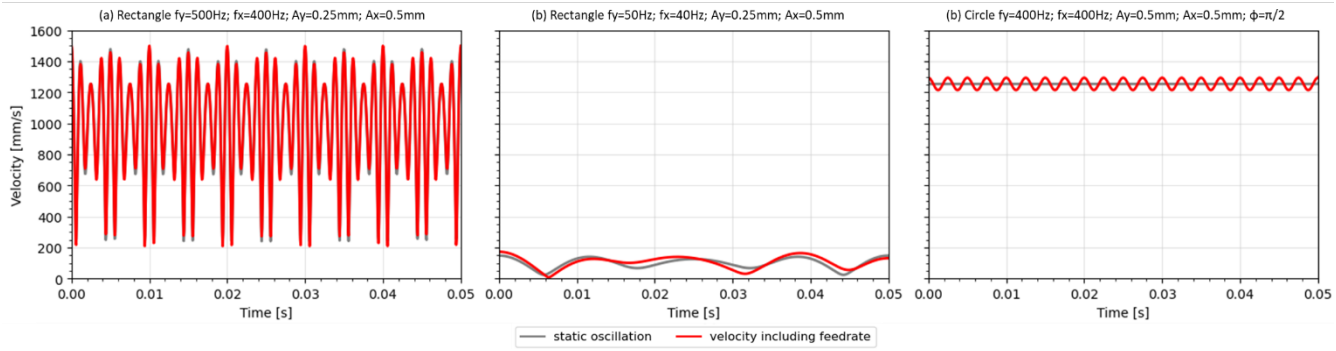

Figure 4: Velocity regimes of different oscillation figures (a) rectangle with >100Hz frequency; (b) rectangle with <100Hz frequency; (b) circle with >100hz frequency

The smaller the amplitudes and frequencies, the smaller the resulting laser beam velocities. At the same time the difference between the fastest and the slowest velocities decreases (figure 4). Depending on the combination of amplitudes, frequencies and phase shift, the oscillation figure and therefore the velocity regime changes significantly. This has a direct impact on the keyhole geometry and the energy deposition into the process. For typical parameter combinations with oscillation frequencies (f_x and f_y between 100 Hz to 2000 Hz) and translation velocities between 10 mm/s and 50 mm/s, the velocity contribution of the linear translation is small (figure 4 (b)). In this case, the keyhole is mostly affected by the dynamics of the beam oscillations. However, this results in a significant variation of the local beam velocities, and this corresponds directly to non-uniform energy input along the trajectory. Without a synchronized control of the laser source, this can lead to excessive or insufficient energy input along the oscillation figure.

Figure 5 shows the energy densities for constant and modulated laser power along the trajectory. The graphs visualize the energy deposition of a Gaussian laser beam on the surface of the work piece and have been calculated in a Python script. For simplicity, uniform absorption of the laser power has been assumed, and heat conduction has been neglected. In reality, the heat dissipation leads to a smearing of the energy input and the energy distribution becomes more uniform below the surface. This homogenization of the absorbed laser energy is more pronounced for materials with high thermal conductivity (Al, Cu). Nevertheless, the different regimes of intensity distribution can be compared and correlated with the metallurgic results.

When applying constant laser power, the energy input at the reversal points (on the side of the weld track) is much higher than in the center, because the velocities are low and therefore the interaction time between energy source and material is high. The opposite phenomenon occurs in the center of the weld track, where the velocities are high (figure 5 (a)). Such a weld establishes a fusion of both plates at the edges, but there is a high likelihood of failure of the connection, because of the limited joining interface. This risk is even more pronounced for wider weld tracks, which would be beneficial to increase mechanical strength of the joint. In the example with constant laser power, the energy density in the reversal point is too high and increased intermixture of the materials starts. Simultaneously the center of the weld track receives too little energy to form a reliable connection. To apply more laser energy therefore is not the preferred solution.

An appropriate modulation of the laser power makes it possible to tailor the intensity distribution for such dissimilar welds. For this purpose, a velocity-controlled modulation (VCM) of the laser power has been implemented into the existing laser controller (FlexiBeam Controller). The VCM-mode calculates the momentary beam velocity during oscillation. The laser

power is adjusted at a rate of 25 kHz to keep the line energy density (the energy deposition per unit length) constant. With appropriate delay settings, the power modulation is synchronized to the position of the laser beam with its corresponding velocity (figure 6 (a)). The required delays of the signal chain amount to 80 µs (±40 µs).

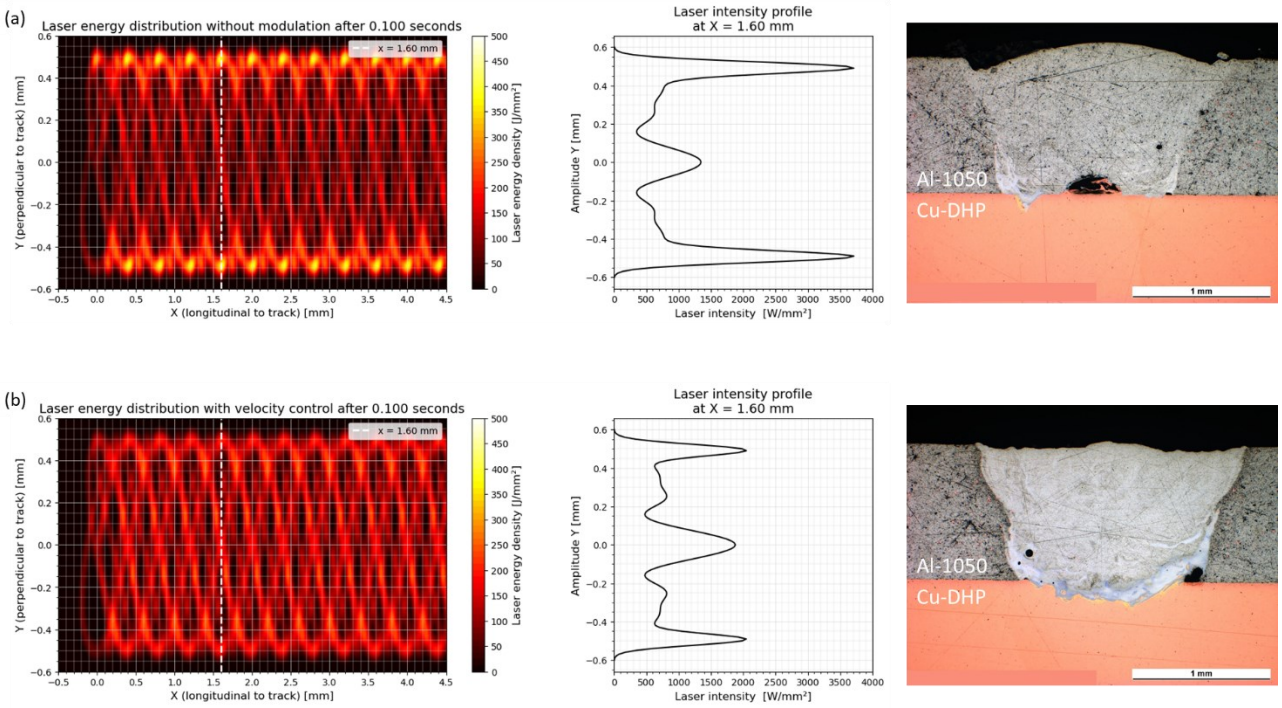

Figure 5: Calculated energy density on the surface of the sample for a rectangle (A_x=0.25; A_y=0.5 mm; f_x=500 Hz; f_y=400 Hz) with beam velocities ranging from 200 mm/s to 1500mm/s with (a) constant laser power; (b) the laser power modulated based on the velocity of the beam

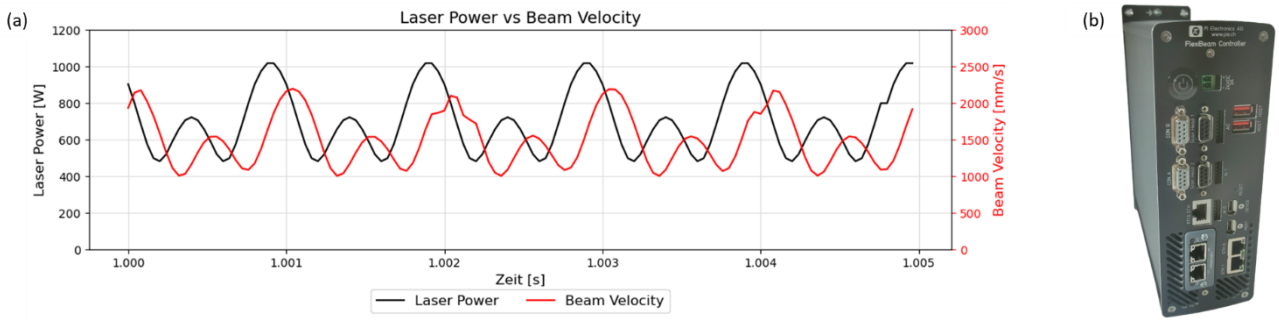

Figure 6: (a) Synchronized and modulated laser power, based on the resulting beam velocity calculated from the mirror positions with the signal delay incorporated; (b) laser power controller

With the modulation of the laser power based on the velocity of the laser beam a uniform energy input along the width of the track can be established (figure 5 (b)). By adjusting the control parameter, the modulation effect can be enhanced or diminished. Figure 5 (b) gives an example of how a velocity-controlled energy input changes the interface between the two dissimilar plates. The cross-section indicates that such a homogenized intensity distribution is as well not the perfect solution. A slightly increased energy input may be beneficial to compensate for higher heat dissipation on the borders of the weld and ensure a uniform shallow depth of molten copper. With an optimization of the control parameters, suitable energy distribution can be achieved.

To demonstrate the application potential of synchronized laser power modulation, experiments have been carried out on samples with aluminum-copper and on steel-copper configuration. The thickness of each metal sheet was 1 mm and the

welded track length 25 mm. The sample was moved below the processing head at velocities ranging from 20 mm/s to 1200 mm/s. The acceleration distance for each velocity was measured and the sample positioned accordingly, to ensure constant velocity in the area of interest. The laser power varied between 400 W and 1900 W. Six oscillation patterns with different amplitude and frequency settings have been examined in a feasibility study (table 2). This work enabled the reduction to ten different Lissajous figures for detailed analysis.

The generic oscillation shapes have been tested with three different velocity-based control modes. For all three control modes and for the uncontrolled setting, the laser power and the velocity of the base trajectory was varied.

Table 2: Variation of intensity distribution of created oscillation figures

Measured intensity	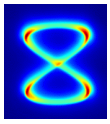	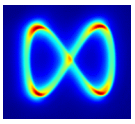	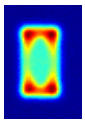	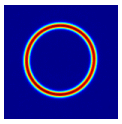	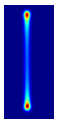	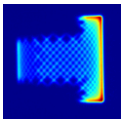
Shape name	standing 8	infinity	Standing rectangle	circle	line	T
Variations investigated	20	20	30	25	42	10
Frequency range	100Hz - 2000Hz	100Hz - 2000Hz	200Hz - 2000Hz	100Hz – 5000Hz	100Hz – 3000Hz	270Hz – 2000Hz
Amplitude range	0.05mm – 0.5mm	0.05mm – 0.5mm	0.1mm – 0.5mm	0.05mm – 0.5mm	0.05mm – 0.5mm	0.1mm – 0.5mm
Power Correction factors (PCF)	Not applied	Not applied	Not applied	Not applied	Not applied	Applied

For analysis, each sample was checked for mechanical connection and accepted for further analysis, when a connection had formed. For metallurgical assessment the samples were cut at two positions (5 mm distance from the sample border on each side) and hot embedded in PolyFast (Struers) powder. Then the samples were grinded and polished (grinded with 320, 500, 800, 1200, 4000 grit silicon carbide foils and polished with 3 µm and 1 µm). The steel-copper samples were etched after the polishing step with V2A-stain (Fem13) according to (Petzow & Carle, 1994). The aluminum-copper samples did not require etching. Each experiment was carried out two to four times. This gives a minimum of four cross-sections per experiment, to ensure reliable interpretation of the results.

3. Results and discussion

3.1. Steel 1.4301 over copper Cu-DHP

Welding steel on copper without shaping or oscillating the laser beam leads to a fine weld with aspect ratios >3:1. For single tracks, the value of the laser energy density (E_A) is relevant for comparison between facilities and different equipment. E_{ST} represents the energy deposited over the irradiated area in [J] per [mm^2].

Equation 2: Energy density E_A

$$E_A = \frac{P_0}{v_t * d_0}$$

With the laser power P_0; the velocity of the trajectory v_t and the diameter of the laser spot d_0.

Starting from an energy density E_A of 50 J*mm^{-2} up to 180 J*mm^{-2} tracks with negligible pores and minimized intermixture of the materials can be achieved. The correlation between weld depth and E_A is not strictly linear. Good tracks are achieved with E_A values ranging from 50 J*mm^{-2} to 100 J*mm^{-2} when using velocities around 300 mm/s. While using velocities of 100 mm/s required E_A values ranging from 100 J*mm^{-2} to 200 J*mm^{-2}.

The thermal conductivity of steel 1.4301 (16.2 W*K^{-1}*m^{-1}) is low compared to aluminum AW-1050A (220 W*K^{-1}*m^{-1}) and Cu-DHP (305 W*K^{-1}*m^{-1}). When welding steel on top of copper, the energy supplied to the process remains more confined to the deposited position and only diffuses comparatively slowly into the surrounding material. By choosing an oscillation pattern with a low velocity spread (range between the highest and lowest velocity of the moving laser beam), the low thermal conductivity helps to stabilize the process. While a circle has the lowest possible velocity spread, the results indicate a stable process with the oscillation pattern “standing 8” and a velocity ratio of ~2.2.

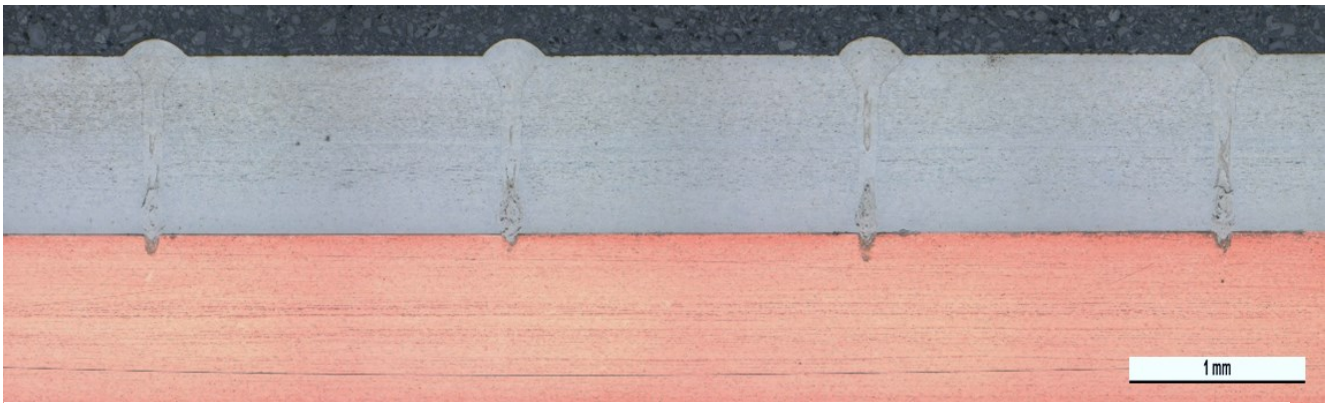

Figure 7: Steel 1.4310 on copper Cu-DHP weld with 200 mm/s velocity and from left to right P_0=850 W; 900 W; 950 W; 1000 W

The “standing 8” oscillation pattern (A_x=0.2 mm; A_y=0.4 mm; f_x=616 Hz; f_y=308 Hz; v_t=31 mm/s) is characterized by a velocity range from 499 mm/s to 1112 mm/s (ratio of ~2.2). Due to the low thermal conductivity, this energy distribution leads to a 0.8 mm wide joining area and limited intermixture of the materials (figure 8). This indicates that one can find appropriate parameter for an oscillations figure, to create dissimilar joints of good quality. Nevertheless, the parameter window is small and the experimental effort to find suitable amplitudes and frequencies must be considered.

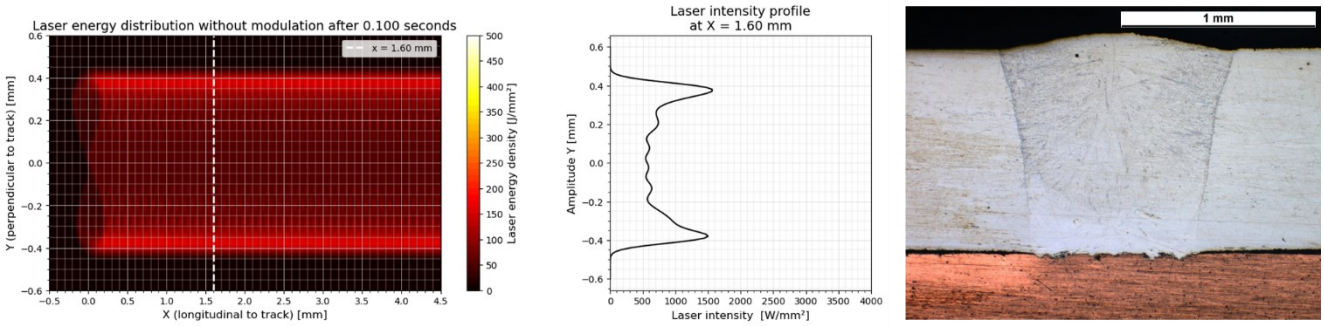

Figure 8: Steel 1.4310 on copper Cu-DHP weld with "standing 8" figure and appropriate energy distribution resulting in a 0.8 mm joint width

3.2. Aluminum AW-1050A over copper Cu-DHP

Welding aluminum on copper without dynamic intensity shaping or oscillating the laser beam leads to a broad weld width compared to weld depth. The thermal conductivity in this case results in a larger melt pool compared to welding steel on copper. Additionally, the difference between the melting temperature of aluminum and copper increases the difficulty to stabilize the process. The energy input must be large enough to just dissolve the surface of the copper. This conflicts with the requirement of achieving minimal intermixture. Consequently, the processing window for acceptable weld connections with thin IMC layer becomes small.

Due to the physical constraints of welding aluminum on copper, the optimum processing parameter range between under- and over-welded joints is small at best. This also holds for welds with superimposed beam oscillation. Using a circular movement with a period of ~1 ms (A_x=0.2 mm; A_y=0.2 mm; f_x=1000 Hz; f_y=1000 Hz; ϕ=90°) and forward trajectory with velocities of v_t=50 mm/s and 100 mm/s joints with limited intermixture can be created (figure 9 (a) and (b)). The amplitudes (A=0.2 mm) result in a joining cross-section of <0.7 mm. Interestingly, the velocity of v_t=50 mm/s creates a larger molten area on the surface on the sample, while the joining cross-section at the contact interface is not significantly increased.

Increasing the amplitude, while maintaining the beam velocity (A_x=0.4 mm; A_y=0.4 mm; f_x=500 Hz; f_y=500 Hz; ϕ=90°; v_t=50 mm/s and 100 mm/s) for the circle figure, increases the joining area to >0.8 mm. Additionally the intermixture of the materials is reduced. However, the larger amplitudes lead to undesired melt pool dynamics (figure 9 (c)).

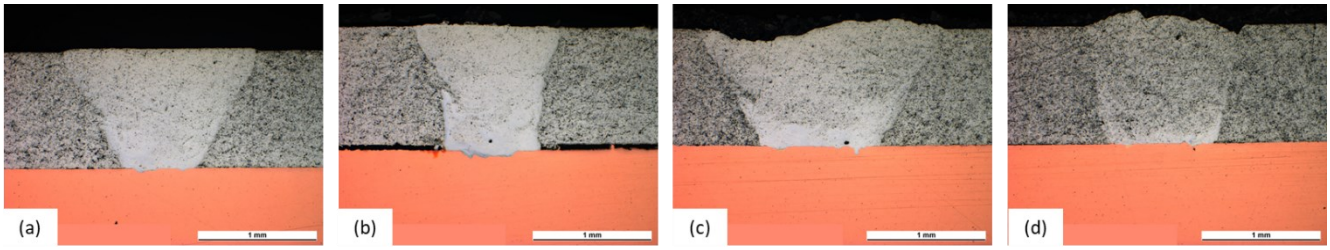

Figure 9: AW-1050A on Cu-DHP with "circle" figure and (a) A_x= A_y=0.2 mm; f_x= f_y=1000 Hz; ϕ=90°; v_t=50 mm/s at P=1200 W; (b) A_x= A_y=0.2 mm; f_x= f_y=1000 Hz; ϕ=90°; v_t=100 mm/s at P=1300 W; (c) A_x= A_y=0.4 mm; f_x= f_y=500 Hz; ϕ=90°; v_t=50 mm/s at P=1400 W; (d) A_x= A_y=0.4 mm; f_x= f_y=500 Hz; ϕ=90°; v_t=100 mm/s at P=1600 W

Switching to a “standing 8” (A_x=0.25 mm; A_y=0.5 mm; f_x=600 Hz; f_y=300 Hz; v_t=50 mm/s) the optimum parameter window is enlarged. Connections with shallow melting of the copper and almost free of pores can be produced in a power range between 1200 W to 1500 W. Nevertheless, such welds show a higher variation of sections with increased thickness of intermetallic phases and sections with thin IMC layers.

The “infinity” oscillation pattern (A_x=0.2 mm; A_y=0.2 mm; f_x=200 Hz; f_y=400 Hz; v_t=50 mm/s) results in the same outcome, as the “standing 8”. The only difference is the reduced cross-section of the joint, due to the smaller amplitude in A_y-direction.

Applying a “standing rectangle” pattern with fixed laser power, only a single parameter set out of 175 different parameter sets created a weld of acceptable quality. When the laser power is controlled based on the velocity, welds of acceptable quality are achieved (figure 10). With a forward trajectory of v_t=40 mm/s, amplitudes of A_x=0.25 mm and A_y=0.5 mm and frequencies of f_x=400 Hz and f_y=320 Hz, joining interfaces of >1.2 mm with minimal IMC content were created. As the results in figure 10 (e) to (h) indicate, there is a reasonably large range of nominal laser power settings for which a good quality can be produced.

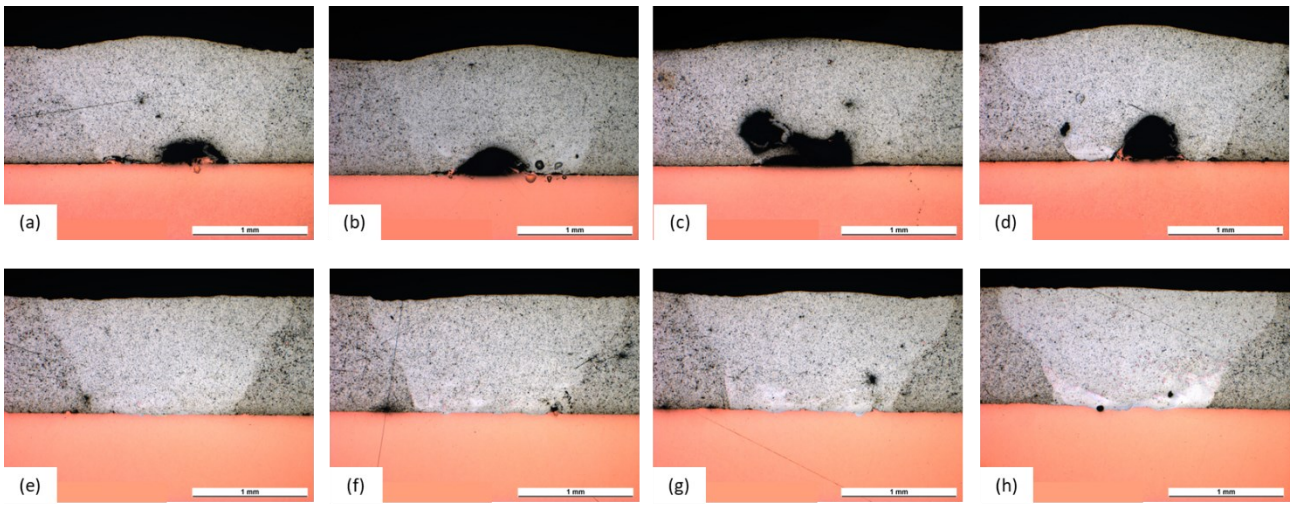

Figure 10: AW-1050A on Cu-DHP with "standing rectangle" figure (A_x=0.25; A_y=0.5 mm; f_x=400 Hz; f_y=320 Hz; v_t=40 mm/s and constant laser power for (a) P=1300 W; (b) P=1400 W; (c) P=1500 W; (d) P=1600 W; and velocity-controlled laser power for (e) P_{avg}=1300 W; (f) P_{avg}=1400 W; (g) P_{avg}=1500 W; (h) P_{avg}=1600 W

Figure 11 is a detailed view of the weld cross section of the joint shown in figure 10 (g). Zone [1] indicates the pure α-aluminum with fine inclusions of eutectic intermixture (α-aluminum with ~1 µm θ-phase inclusions [2]). Zones [2] are purely eutectic regions and zones [3] have larger θ-phase dendrites with eutectic intermixture in between. These pure θ-phase layer ranges in thickness from below 1 µm to 15 µm with an average thickness below 10 µm. Based on the research by (Solchenbach et al., 2014), this indicates an electrical resistance of the joint slightly above the base material.

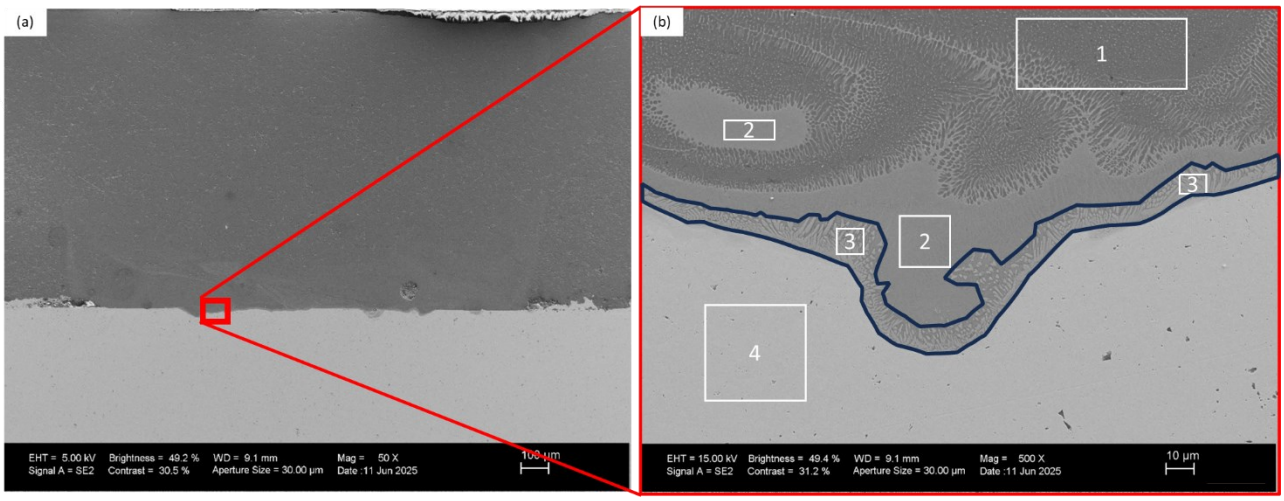

Figure 11: (a) Cross section of weld track; (b) detailed view of the weld cross section with thin θ-phase layer (3-blue frame), further (1) α-aluminum and eutectic phase, (2) eutectic phase, (3) θ-phase and eutectic phase (4) copper

4. Conclusion

The work presented in this conference paper comprises the creation of different intensity distributions for laser keyhole welding of aluminum – copper and steel – copper joints. The experiments resulted in a significant increase of the joining area and a considerable reduction of the intermetallic phases in the weld zone, when dynamic beam shaping was applied. The main conclusions from this work are:

- Controlling the thermal distribution is the key to welding dissimilar materials over an increased joining area with reduced intermixture.
- Laser welding with spatial and temporal laser intensity shaping increases process flexibility and robustness and is therefore beneficial for producing dissimilar weld joints of high quality
- Commercially available scanners offer high flexibility and sufficient dynamics to optimize the energy input for laser keyhole welding
- Synchronized laser power modulation – particularly a velocity-controlled energy input - helps to achieve reliable connections between dissimilar materials

5. Outlook

This work represents the first work packages of a larger project to optimize laser welding of dissimilar materials and improve process robustness. More work is required to establish reliable correlation between the different processing parameter combinations and the resulting electrical and mechanical properties of the welded joints. In combination with the synchronized laser power modulation, a large variety of other intensity distributions remain to be explored. In order to keep the experimental effort manageable, more advanced simulation tools must be developed to guide the experiments. Ultimately this will be combined with a fast closed-loop control system to increase process robustness.

Acknowledgments

This project was done in close cooperation between *FHNW* and the *Technische Universität Ilmenau*. We gratefully acknowledge the financial support from the *Swiss Innovation Agency Innosuisse*.

References

Braunovic, M., & Alexandrov, N. (1994). Intermetallic compounds at aluminum-to-copper electrical interfaces: Effect of temperature and electric current. IEEE Transactions on Components, Packaging, and Manufacturing Technology: Part A, 17(1), 78–85. https://doi.org/10.1109/95.296372

Das, A., Li, D., Williams, D., & Greenwood, D. (2018). Joining Technologies for Automotive Battery Systems Manufacturing. World Electric Vehicle Journal, 9(2), Article 2. https://doi.org/10.3390/wevj9020022

Dimatteo, V., Ascari, A., & Fortunato, A. (2019). Continuous laser welding with spatial beam oscillation of dissimilar thin sheet materials (Al-Cu and Cu-Al): Process optimization and characterization. Journal of Manufacturing Processes, 44, 158–165. https://doi.org/10.1016/j.jmapro.2019.06.002

Fetzer, F., Jarwitz, M., Stritt, P., Weber, R., & Graf, T. (2016). Fine-tuned Remote Laser Welding of Aluminum to Copper with Local Beam Oscillation. Physics Procedia, 83, 455–462. https://doi.org/10.1016/j.phpro.2016.08.047

Haug, P., Seebach, J., Hesse, T., & Speker, N. (2019). Beam shaping BrightLine Weld: Latest application results. High-Power Laser Materials Processing: Applications, Diagnostics, and Systems VIII, 9.

International Energy Agency. (2023). Energy Technology Perspectives 2023. Energy Technology Perspectives.

Jarwitz, M., Fetzer, F., Weber, R., & Graf, T. (2018). Weld Seam Geometry and Electrical Resistance of Laser-Welded, Aluminum-Copper Dissimilar Joints Produced with Spatial Beam Oscillation. Metals, 8(7), Article 7. https://doi.org/10.3390/met8070510

Klocke, F., Schulz, M., & Gräfe, S. (2017). Optimization of the Laser Hardening Process by Adapting the Intensity Distribution to Generate a Top-hat Temperature Distribution Using Freeform Optics. Coatings, 7(6), 77–93. https://doi.org/10.3390/coatings7060077

Leitz, A. (2016). Laserstrahlschweißen von Kupfer- und Aluminiumwerkstoffen in Mischverbindung. Herbert Utz Verlag.

Marbach, M., Gärtner, F., Daetwyler, R., Julius, M., & Hoebel, M. (2023, June 27). Controlled laser hardening and laser metal deposition with flexible beam shaping. Lasers in Manufacturing Conference 2023, München.

Möbus, M., & Woizeschke, P. (2023). Keyhole-in-keyhole formation by adding a coaxially superimposed single-mode laser beam in disk laser deep penetration welding. Welding in the World, 67(6), 1467–1478. https://doi.org/10.1007/s40194-023-01484-9

Nahr, F., Bartels, D., Rothfelder, R., & Schmidt, M. (2023). Influence of Novel Beam Shapes on Laser-Based Processing of High-Strength Aluminium Alloys on the Basis of EN AW-5083 Single Weld Tracks. Journal of Manufacturing and Materials Processing, 7(3), Article 3. https://doi.org/10.3390/jmmp7030093

Norouzian, M., Amne Elahi, M., & Plapper, P. (2023). A review: Suppression of the solidification cracks in the laser welding process by controlling the grain structure and chemical compositions. Journal of Advanced Joining Processes, 7, 100139. https://doi.org/10.1016/j.jajp.2023.100139

Petzow, G., & Carle, V. (1994). Metallographisches, keramographisches, plastographisches Ätzen (6., vollständig überarbeitete Auflage). Borntraeger.

Pfeifer, S., Großmann, S., Freudenberger, R., Willing, H., & Kappl, H. (2012). Characterization of Intermetallic Compounds in Al-Cu-Bimetallic Interfaces. 2012 IEEE 58th Holm Conference on Electrical Contacts (Holm), 1–6. https://doi.org/10.1109/HOLM.2012.6336554

Ponweiser, N., Lengauer, C. L., & Richter, K. W. (2011). Re-investigation of phase equilibria in the system Al–Cu and structural analysis of the high-temperature phase η1-Al1−δCu. Intermetallics, 19(11), 1737–1746. https://doi.org/10.1016/j.intermet.2011.07.007

Prieto, C., Vaamonde, E., Diego-Vallejo, D., Jimenez, J., Urbach, B., Vidne, Y., & Shekel, E. (2020). Dynamic laser beam shaping for laser aluminium welding in e-mobility applications. Procedia CIRP, 94, 596–600. https://doi.org/10.1016/j.procir.2020.09.084

Sadeghian, A., & Iqbal, N. (2022). A review on dissimilar laser welding of steel-copper, steel-aluminum, aluminum-copper, and steel-nickel for electric vehicle battery manufacturing. Optics & Laser Technology, 146, 107595. https://doi.org/10.1016/j.optlastec.2021.107595

Solchenbach, T., & Plapper, P. (2013). Combined Laser Beam Braze-Welding Process for Fluxless Al-Cu Connections. Proceedings of the COMA, 13.

Solchenbach, T., Plapper, P., & Cai, W. (2014). Electrical performance of laser braze-welded aluminum–copper interconnects. Journal of Manufacturing Processes, 16(2), 183–189. https://doi.org/10.1016/j.jmapro.2013.12.002

Touloukian, Y. S. (1973). Thermophysical properties of matter Vol.7—Metals and alloys (Vol. 7). IFI/Plenum. https://apps.dtic.mil/sti/citations/ADA951941

Wagner, J., Heider, A., Ramsayer, R., Weber, R., Faure, F., Leis, A., Armon, N., Susid, R., Tsiony, O., Shekel, E., & Graf, T. (2022). Influence of dynamic beam shaping on the geometry of the keyhole during laser beam welding. Procedia CIRP, 111, 448–452. https://doi.org/10.1016/j.procir.2022.08.185

Zwicker, M. F. R., Moghadam, M., Zhang, W., & Nielsen, C. V. (2020). Automotive battery pack manufacturing – a review of battery to tab joining. Journal of Advanced Joining Processes, 1, 100017. https://doi.org/10.1016/j.jajp.2020.100017